Polycyclic aromatic hydrocarbons (PAHs) levels in PM_{10} and bulk deposition using Mosspheres: A pilot study in an urban environment

Carme Pacín [a,*], Javier Martínez-Abaigar [b], Encarnación Núñez-Olivera [b], Jesús R. Aboal [a], Flavia De Nicola [c], J. Ángel Fernández [a]

[a] *CRETUS Center, Department of Functional Biology, Ecology Unit, Universidade de Santiago de Compostela, 15782, Santiago de Compostela, Spain*
[b] *Faculty of Science and Technology, Universidad de La Rioja, Madre de Dios 53, 26006, Logroño Spain*
[c] *Department of Sciences and Technologies, Università degli Studi del Sannio di Benevento, 82100, Benevento, Italy*

ARTICLE INFO

ABSTRACT

Study air polycyclic aromatic hydrocarbons (PAHs) capturing the spatial variability of their concentrations is not economically feasible with conventional methods. In the present work we tested, for the first time and under real conditions, the suitability for intensive monitoring and mapping these contaminants of innovative, cost-effective passive air samplers known as "Mosspheres". The Mosspheres, filled with a devitalised *Sphagnum palustre* L. moss clone, were placed in a 575 m. grid in a medium-sized European city for three months. Concentrations in the moss tissues of 15 priority PAHs, including benzo(a)pyrene, were determined and converted into PM_{10} and bulk deposition with the equations proposed in a recent study. Low concentrations of PAHs were detected, with only a few enriched points never exceeding the legal thresholds, near industrial areas and busy roads. Despite these low PAH concentrations, Mosspheres were able to detect spatial structure for several PAHs and high-resolution pollution maps were constructed for these compounds. The results prove the high sensitivity and suitability of Mosspheres for mapping PAH levels and for quantitative (i.e. PAHs with 4 or more rings) and qualitative (3-ring PAHs) monitoring. Thus, this study supports their widespread application and its potential inclusion in European Directives on air quality control.

1. Introduction

Polycyclic aromatic hydrocarbons (PAHs) are organic pollutants with two or more benzene rings. These compounds are emitted to the atmosphere during the pyrolysis and incomplete combustion of fossil fuels and biomass (Wang et al., 2013). Major worldwide sources of atmospheric PAHs include vehicular traffic, domestic heating and industrial processes, although natural sources such as wildfires and volcanic eruptions are also important (Patel et al., 2020; Shimada et al., 2022; Wu et al., 2023). In the atmosphere, low molecular weight PAHs (2- and 3-ring PAHs) are mainly distributed in the gaseous phase, while heavier PAHs tend to be associated with particulate matter (Ma et al., 2013; Zhan et al., 2022).

Some PAHs, especially those of high molecular weight, are of particular concern due to their potentially toxic effects, which include potentially strong carcinogenic and genotoxic effects (Montaño-Soto and Garza-Ocañas, 2014; Patel et al., 2020). This concern, together with the high persistence and mobility in the atmosphere and the capacity of PAHs to be biomagnified in food webs, has prompted governments to establish legislation regarding emissions of these compounds (Kim et al., 2013; Ravindra et al., 2008; Verbruggen, 2012). Thus, European Directive 2004/107/EC (European Parliament and the Council of the European Union, 2004) established that average concentrations for 1 year of measurement should not exceed 1 ng m^{-3} of benzo(a)pyrene in particulate matter of diameter up to 10 μm (PM_{10}). Although this Directive states that other important PAHs such as benzo(a)anthracene, benzo(b)fluoranthene and benzo(j)fluoranthene should also be measured in both PM_{10} and bulk deposition (BD), no additional target values were established because benzo(a)pyrene was considered an indicator of the remaining PAHs. Moreover, in the US, the Environmental Protection Agency (EPA) considers 16 PAHs as priority pollutants, while the Occupational Safety and Health Administration (OSHA) established an 8-h time-weighted average exposure limit of 200 ng m^{-3} in workplace air.

To ensure that these levels are not exceeded, direct monitoring methods with active air samplers and BD collectors are frequently used

---

* Corresponding author.
  E-mail address: mcarme.pacin@usc.es (C. Pacín).

to measure PAHs in PM_{10} and BD respectively. However, the technical equipment required and the high cost of implementation limit measurements to a few monitoring stations that barely cover the study areas (Augusto et al., 2013; Harmens et al., 2007). These limitations have led to the adoption of passive sampling techniques, such as polyurethane foam disks (PUF), which are cheaper and maintenance-free, and allow intensive urban monitoring networks to be established (Aslam et al., 2022; Estellano et al., 2012; Thang et al., 2020). These networks have enabled predictive mapping of pollution, by providing high spatial resolution data on air quality and identifying pollution hotspots (Choi et al., 2012; Qu et al., 2021; Thang et al., 2020).

Another approach that is commonly used to monitor PAHs is the use of organisms as biomonitors. In urban areas, mosses have been widely used for this purpose (Capozzi et al., 2020; Carrieri et al., 2021; Martinez-Swatson et al., 2020; Vingiani et al., 2015). However, despite the well-documented capacity of moss for detecting pollution hotspots and mapping pollution (Ares et al., 2011; Jovan et al., 2021), the concentrations of pollutants in moss tissues do not provide quantitative measurements of the concentrations in PM_{10} and BD, thus limiting their usefulness for regulatory purposes and health risk assessment. In an attempt to resolve this limitation, a new biotechnological tool, the "Mossphere®", was developed in the European "MOSSclone" project (FP7. ENV. 2011-Eco-Innovation: www.mossclone.eu; Patent EP3076171A1; WO2016156443-A1). This original device, filled with a devitalised moss clone, takes up chemical pollutants which bind to the moss cell wall by purely physic-chemical processes (Capozzi et al., 2016). As a result, Aboal et al. (2020) have found, by deploying conventional methods and Mosspheres at the same time in several sampling points, for different climates, seasons and environments, significant correlations between the concentrations of PAHs with 4 or more rings in Mosspheres filled with the moss *Sphagnum palustre* and those measured in PM_{10} and BD. The Mossphere has thus become the first biomonitor in which the PAH concentrations are related to the concentrations measured by conventional methods (Aboal et al., 2020). However, despite these promising advances, neither these devices, which are cost-effective and environmentally friendly (see Alfonsín et al., 2015), nor the expressions relating their concentrations to PM_{10} and BD, have been applied to monitor and mapping PAH levels in an entirely study area.

In the present study we considered these theoretical advances in testing the capacity of Mosspheres to monitor and map PAH levels in PM10 and BD under real conditions, using a regular urban network of Mosspheres located in a medium-sized European city of ca. 200,000 inhabitants as a working example.

2. Material and methods

2.1. Mossphere devices

Mosspheres were prepared at the laboratory. Each Mossphere device consists of two concentric spheres: an inner sphere of diameter 10 cm made of high-density polyethylene and an external sphere of diameter 11 cm made from nylon netting of mesh size 2 mm. The *Sphagnum palustre* L. clone was grown in bioreactors following the method of Beike et al. (2014). The moss thus obtained was washed with water and EDTA before being devitalised in an oven in three consecutive drying cycles of 8 h, each at 50, 80 and 100 °C. Aliquots of 3 g of prepared moss were inserted in the space between the two spheres (10 mm wide), to produce a ratio between the moss weight and the surface area of the bag of 10 mg cm^{-2} (Capozzi et al., 2016). The prepared Mosspheres were stored in vacuum-sealed polyethylene bags until exposure.

2.2. Exposure of Mosspheres

The present study was carried out in the city of Logroño (N Spain; 42°28′12″N latitude, 2°26′44″W longitude, 384 m altitude). This city

has a continental Mediterranean climate and is urbanistically similar to many other European cities, with widely distributed residential areas (ca. 155,000 inhabitants in the city and a total of ca. 197,000 in the metropolitan area). Industrial activity, mainly involving the food and automotive industries, is concentrated in two industrial parks located in the outskirts of the city (Fig. 1). There are also some tunnels and busy roads, with some hotspots of heavy traffic.

Eighty-four Mosspheres (one in each sampling point) were exposed at height of 4 m (most were attached to streetlights on fiberglass poles) during three months (March to May 2018). This height and exposure time were selected following the last recommendations in moss biomonitoring (Ares et al., 2012; Capozzi et al., 2016). Seventy-eight of them were distributed in a regular grid of side 575 m, covering the whole city. Six additional spheres were placed in sites in the urban periphery. The sampling network covered the existing variety of the city's structures, with sampling points in industrial areas, residential areas, quarries, green areas or roads (see Fig. 1 for more information about each sampling point). Three samplers (numbers 7, 74, and 84) were lost during the exposure period.

After 91 days of exposition, the Mosspheres were collected, placed in polyethylene zipper bags and transported to the laboratory. In addition, five Mosspheres, that were kept in the laboratory inside the vacuum-sealed bags involved in aluminium foil during these 3 months, were taken out of the sealed bags and carried in polyethylene zipper bags to all sampling points the day of the collection of the exposed Mosspheres, to check for possible contamination during the transport. The PAHs concentrations determined in these samplers were considered the control concentration. Moreover, the mean PAHs concentrations in the moss of 5 unexposed Mosspheres were considered the initial concentration (t_0).

Once in the laboratory, the moss material was pulled out manually from the Mosspheres, oven-dried (24 h at 40 °C) and pulverized in a tangential mill (Restch MM-400, with zirconium oxide vessels) and stored in amber vials until PAH analyses.

2.3. Chemical analysis

For all Mosspheres (t_0, controls, and exposed samples), the PAHs content of the moss material was extracted by matrix solid-phase dispersion extraction. Briefly, PAHs were eluted using hexane, dichloromethane and Na_2SO_4 and applying a pressure program from 640 mbar to 210 mbar during 40 min. Then, 20 μl of internal standard was added. The extract was analysed by programmed temperature vaporisation-gas chromatography-tandem mass spectrometry (PTV-GC-MS/MS) determination using a Trace-GC-Polaris Q, Thermo-Finningan and the Xcalibur software. The concentrations of the following PAHs were determined: acenaphthene (Ace); fluorene (F); phenanthrene (P); anthracene (Ant); fluoranthene (Fl); pyrene (Pyr); benzo[a]anthracene (BaAnt); chrysene (Chr); benzo[b+j]fluoranthene (BbjFl); benzo[k]fluoranthene (BkFl); benzo[e]pyrene (BePyr); benzo[a]pyrene (BaPyr); dibenzo[a,h]anthracene (DBahAnt); indene[1,2,3-cd]pyrene (Ipyr); and benzo[ghi]perylene (BghiPer). Procedural and instrumental blanks were systematically evaluated with each batch of samples. For further details regarding the chemical analysis see Concha-Graña et al. (2015).

2.4. Analytical quality results

Analytical quality control was performed by two parallel analyses. First, the limit of quantification (LOQ) of each compound was calculated from the blanks as ten times the standard deviation of their values (Table 1). In general, between 0 and 16% of the samples were found to be below the LOQ and these concentrations were substituted by 0.5 * LOQ. In the case of DBahAnt, 51% of the samples were below this limit, and this compound was therefore excluded from the PM_{10} and BD estimation. Secondly, percent recoveries of 6 deuterated compounds (phenanthrene D10, fluoranthene D8, pyrene D10, chrysene D12, benzo
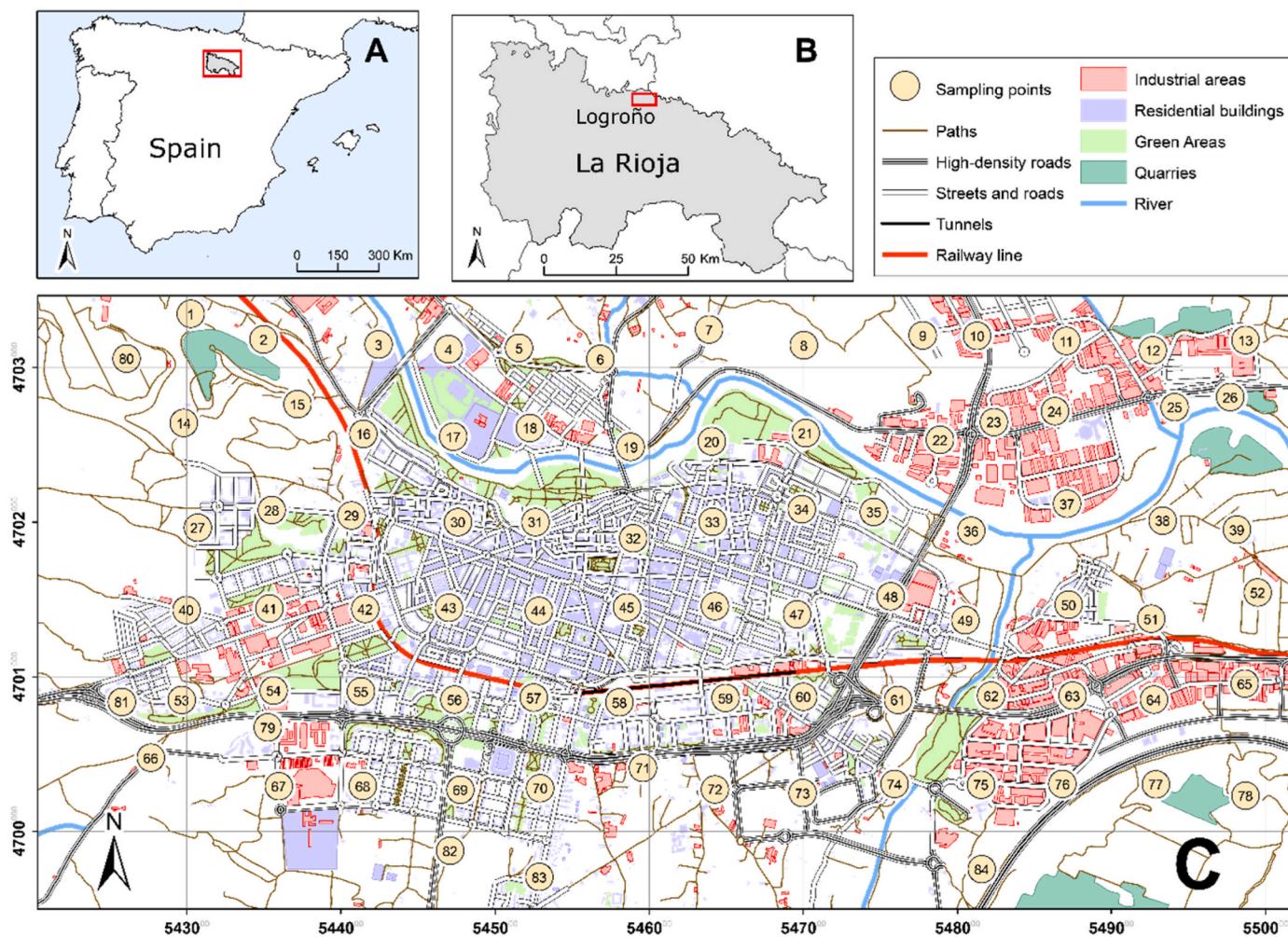
Fig. 1. Location of the city where the PAH monitoring was carried out and of the Mossphere samplers. Location of the province (La Rioja) and the city surveyed (Logroño) in Spain (Fig. 1A, 1.B). Detailed map showing the city structure and the sampling points where the Mosspheres were located. The sampling grid consisted of 84 points: 78 in a regular grid (of side 575 m), and six additional points in the periphery (79–84). Three of the Mosspheres (numbers 7, 74, and 84) were lost during the exposure period (Fig. 1C).

Table 1
Limits of quantification (LOQ), percentage of Mossphere samples determined below these values.

Compound	LOQ (ng g^{-1})	samples < LOQ (%)
Ace	1.1	1
F	0.2	0
P	1.7	2
Ant	1.2	3
Fl	1.0	0
Pyr	1.2	0
BaAnt	0.2	8
Chr	0.2	1
BbjFl	0.4	3
BkFl	0.4	9
BePyr	0.3	11
BaPyr	0.5	12
DBahAnt	1.0	51
Ipyr	0.1	16
BghiPer	0.8	3

Ace, acenaphthene; F, fluorene; P, phenanthrene; Ant, anthracene; Fl, fluoranthene; Pyr, pyrene; BaAnt, benzo[a]anthracene; Chr, chrysene; BbjFl, benzo[b+j]fluoranthene; BkFl, benzo[k]fluoranthene; BePyr, benzo[e]pyrene; BaPyr, benzo[a]pyrene; DBahAnt, dibenzo[a,h]anthracene; Ipyr, indene[1,2,3-cd]pyrene; BghiPer, benzo[ghi]perylene.

[a]pyrene D12, benzo[ghi]perylene D12) added before the extraction were calculated, ranging from 70% to 103%, and included in calculations to quantify all the investigated PAHs. Similar procedures were previously reported by several authors (Carrieri et al., 2021; Pérez-Fernández et al., 2018).

2.5. Data treatment and statistical analysis

Contamination of the samples during transportation to the laboratory in the polyethylene zipper bags was discarded by comparing the PAHs concentrations in t_0 and in the controls (Mann-Whitney *U* test, wilcox.test function in R Core). The method developed by Aboal et al. (2020) was used to estimate the PAH concentrations (of 4-, 5-, and 6-rings, their sums, and total PAHs) in BD and PM$_{10}$. PAH deposition was estimated as follows: Deposition$_{moss}$= (C*M$_{moss}$)/(A*t) (where C is the PAH concentration in moss (μg g^{-1}), M$_{moss}$ is the amount (g) of moss exposed in each sphere (3 g), A is the surface area (0.0346 m^2) of the Mossphere, and t is the exposure time (91 days)). Flux of PAHs in the air was estimated in this way: Flux$_{moss}$ = (C*M$_{moss}$)/(V*t), where C is the PAH concentration in moss (ng g^{-1}), M$_{moss}$ is the amount (3 g) of moss exposed in each sphere, V is the rate of air volume in contact with the Mossphere (1.666 m^3 day^{-1}, estimated by Aboal et al. (2020) from estimates of other passive samplers), and t is the exposure time (91 days). Then, Deposition$_{moss}$ was transformed into BD (μg m^{-2} day) and Flux$_{moss}$

(ng m^{-3}) into PM$_{10}$ using the equations shown in Table 1SM, derived from Aboal et al. (2020). Transformations of the 3-ring PAHs concentrations determined in the Mosspheres into PM$_{10}$ and BD and of BaAnt into PM$_{10}$ were ruled out, because of the lack of significant correlations (Aboal et al., 2020).

Some PAH diagnostic ratios were applied to the BD PAH concentrations (i.e. BaAnt/(BaAnt + Chr); Fl/(Fl + Pyr); Ipyr/(Ipyr + BghiPer)) (Yunker et al., 2002). Since each source of PAHs has characteristic ranges of these ratios, they should help to identify PAHs emission sources.

The PM$_{10}$ and BD concentrations were weighted according to the toxicity, using the toxic BaPyr equivalency factor (TEF) (Environment Protection Authority, 2021; Nisbet and Lagoy, 1992) (Table 2). The concentrations of each compound were multiplied by their respective TEF values, to yield the toxic BaPyr equivalent concentrations (TEQ).

Descriptive statistics, density functions, omnidirectional semivariograms and ordinary kriging were performed in R using the R Core and the packages "ggplot2", "sp" and "gstat" (Bivand et al., 2013; Gräler et al., 2016; Wickham, 2009). Pollution maps were constructed using ArcMap 10.7 (ESRI©).

3. Results

3.1. PAH levels

The median PAH concentrations in the Mosspheres and the corresponding estimated concentrations in BD and PM$_{10}$, together with their interquartile ranges (IQR), are shown in Table 2 (see PAH concentrations in Mosspheres, BD and PM$_{10}$ at each sampling point in Table 2SM). The total median concentration of 3-ring PAHs in Mosspheres (0.057 µg g^{-1}) was higher than the sums of the 4-ring, 5-ring and 6-ring PAHs, while the reverse was found for the estimated PM$_{10}$ and BD, with the sum of the 6-ring PAHs (0.077 µg m^{-2} day^{-1} in BD and 0.294 ng m^{-3} in PM$_{10}$) being the highest. When the concentration of each compound was weighted according to the TEF, the highest TEQ values were obtained for BaPyr and BbjFl in BD and for Ipyr and BaPyr in PM$_{10}$ (Table 2).

For the estimated concentrations of PAHs in PM$_{10}$ (Fig. 2) and BD (Fig. 1SM), kernel density diagrams revealed a first component (background level) in which the vast majority of the data were included. In a

few instances, the concentrations were higher than the modal value, implying the existence of some enriched stations, 8 of them consistently enriched for most PAHs. Four of these stations were located in the SE part of the territory studied (Fig. 1), either in an industrial park (63 and 75) or near a motorway (77 and 78); one in the NE part, in another industrial park (22); two in the W zone (40 and 66), one in the SW near a gravel extraction area with heavy lorry traffic (66); and one in a public car park in the centre of the city (47). For 6-ring PAHs (i.e. Ipyr and BghiPer, and the total 6-ring sum), together with the stations already mentioned, PAH levels were highest at stations number 22, number 12 (located in the industrial park in the NE of the city) and number 18 (near a public parking in the N part). When the totality of PAHs were considered, the most enriched station was clearly number 47. This is because the 3-ring PAHs determined in the Mosspheres, whose transformation into PM$_{10}$ and BD was discarded, were taken into account for total PAHs concentration transformation.

3.2. Spatial structure of PAH concentrations

Although the stations with high PAH levels were mainly located in particular sites (industrial areas and near car parks or busy roads), significant increases ($p < 0.05$) in the variance with distance, i.e. spatial structure, were only observed in both PM$_{10}$ and BD in the omnidirectional semivariograms for Pyr, BaPyr, BePyr, BghiPer and the sums of 5- and 6-ring PAHs (Fig. 2 and 3SM). The kriging maps obtained for these PAHs were similar, all showing a main source of pollution in the industrial park and the motorway located in the SE part of the city (see Fig. 3 for BaPyr, Fig. 4 for Pyr and Figs. 4–7SM for, respectively, BePyr, BghiPer and the sums of 5- and 6-ring PAHs in PM$_{10}$). Other smaller areas with high PAH levels were located in the SW (especially for BaPyr, BePyr and the sum of 5-ring PAHs) and NE (for Pyr, BaPyr, BghiPer and the sum of 6-ring PAHs) of the map, for the reasons given above. Other small but defined spots of pollution close to other industrial areas, car parks and busy roads were also detected for Pyr, BaPyr and the sum of 5-ring PAHs.

Finally, no detectable pattern was observed in the diagnostic ratios used (BaAnt/(BaAnt + Chr); Fl/(Fl + Pyr) and Ipyr/(Ipyr + BghiPer)). This way, it was not possible to identify the PAHs pollution emission sources, which supports the existence of diffuse pollution sources.

Table 2
Median concentrations of PAHs in Mosspheres and corresponding estimated concentrations in bulk deposition (BD) and PM$_{10}$, together with interquartile ranges and their toxic equivalence. IQR: Interquartile range; TEF: BaPyr toxic equivalence factor; TEQ: BaPyr toxic equivalent concentrations. See section 2.5 for further details regarding transformation of Mosspheres concentration into BD and PM$_{10}$.

Compound	TEF	Mosspheres (µg g^{-1})		BD (µg m^{-2} d^{-1})			PM$_{10}$ (ng m^{-3})		
		Median	IQR	Median	IQR	TEQ	Median	IQR	TEQ
Ace	0.001	0.007	0.013	–	–		–	–	
F	0.001	0.015	0.013	–	–		–	–	
P	0.001	0.028	0.011	–	–		–	–	
Ant	0.01	0.004	0.003	–	–		–	–	
Fl	0.001	0.012	0.008	0.002	0.007	0.000002	0.016	0.012	0.000016
Pyr	0.001	0.012	0.011	0.007	0.017	0.000007	0.022	0.035	0.000022
BaAnt	0.1	0.001	0.001	0.001	0.001	0.0001	–	–	–
Chr	0.01	0.005	0.003	0.002	0.002	0.00002	0.027	0.017	0.00027
BbjFl	0.1	0.007	0.004	0.045	0.048	0.0045	0.120	0.075	0.012
BkFl	0.1	0.002	0.001	0.004	0.003	0.0004	0.019	0.010	0.0019
BePyr	1.0	0.002	0.004	0.002	0.005	0.002	0.006	0.036	0.006
BaPyr	1.0	0.003	0.002	0.009	0.006	0.009	0.039	0.061	0.039
DBahAnt	5.0	0.001	0.002	–	–	–	–	–	–
Ipyr	0.1	0.003	0.004	0.006	0.009	0.0009	0.061	0.127	0.061
BghiPer	0.01	0.009	0.010	0.014	0.016	0.00016	0.285	0.214	0.00285
3-rings		0.057	0.034	–	–		–	–	
4-rings		0.030	0.023	0.014	0.035		0.048	0.093	
5-rings		0.016	0.012	0.053	0.066		0.239	0.252	
6-rings		0.013	0.013	0.077	0.094		0.294	0.359	
Total		0.122	0.072	0.142	0.205		0.541	0.536	

Ace, acenaphthene; F, fluorene; P, phenanthrene; Ant, anthracene; Fl, fluoranthene; Pyr, pyrene; BaAnt, benzo[a]anthracene; Chr, chrysene; BbjFl, benzo[b+j]fluoranthene; BkFl, benzo[k]fluoranthene; BePyr, benzo[e]pyrene; BaPyr, benzo[a]pyrene; DBahAnt, dibenzo[a,h]anthracene; Ipyr, indene[1,2,3-cd]pyrene; BghiPer, benzo[ghi]perylene. ∑4-ring, ∑5-ring, ∑6-ring, sum of 4-, 5- and 6-ring PAH concentrations. Total: sum of all compounds determined.

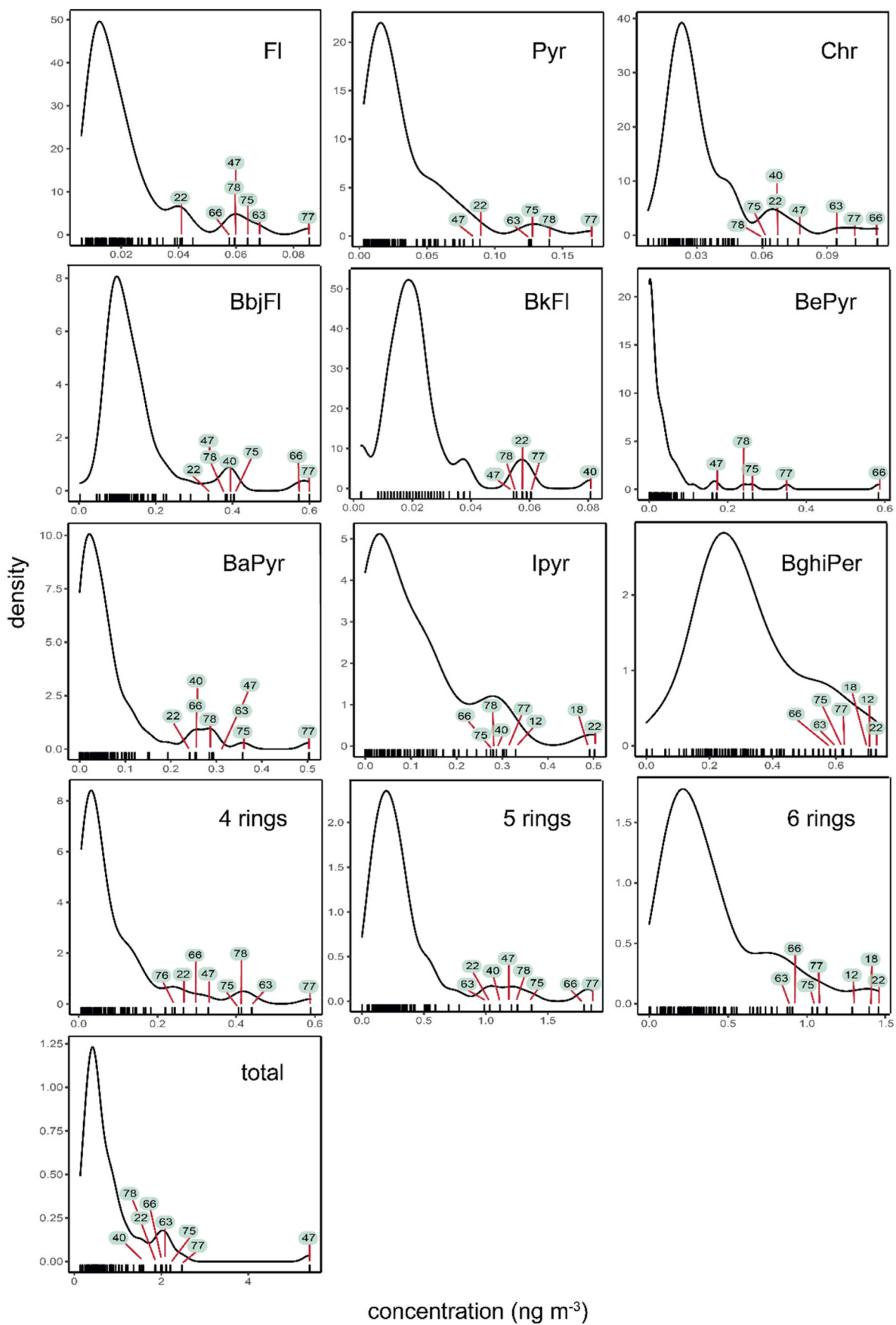**Fig. 2.** Distribution of estimated PAH levels (ng m^{-3}) in PM$_{10}$. Kernel smoothing of the data from the 81 sampling points. The red lines indicate the PAH levels at different sampling stations shown inside the green circles.
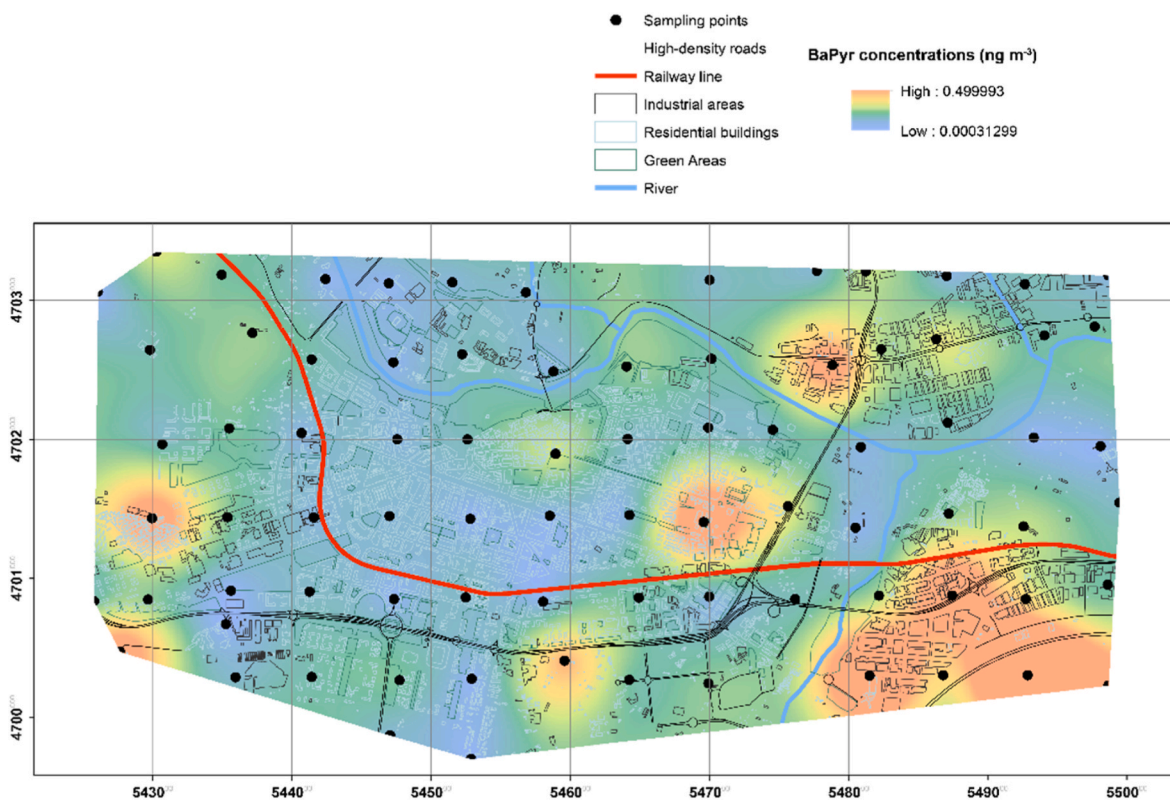
Fig. 3. Pollution map for the city of Logroño (N Spain). The map was produced by kriging of benzo(a)pyrene (BaPyr) concentrations in PM_{10} (ng m^{-3}) estimated from the concentrations determined in Mosspheres. Reddish and bluish tones represent higher and lower levels of this compound, respectively.
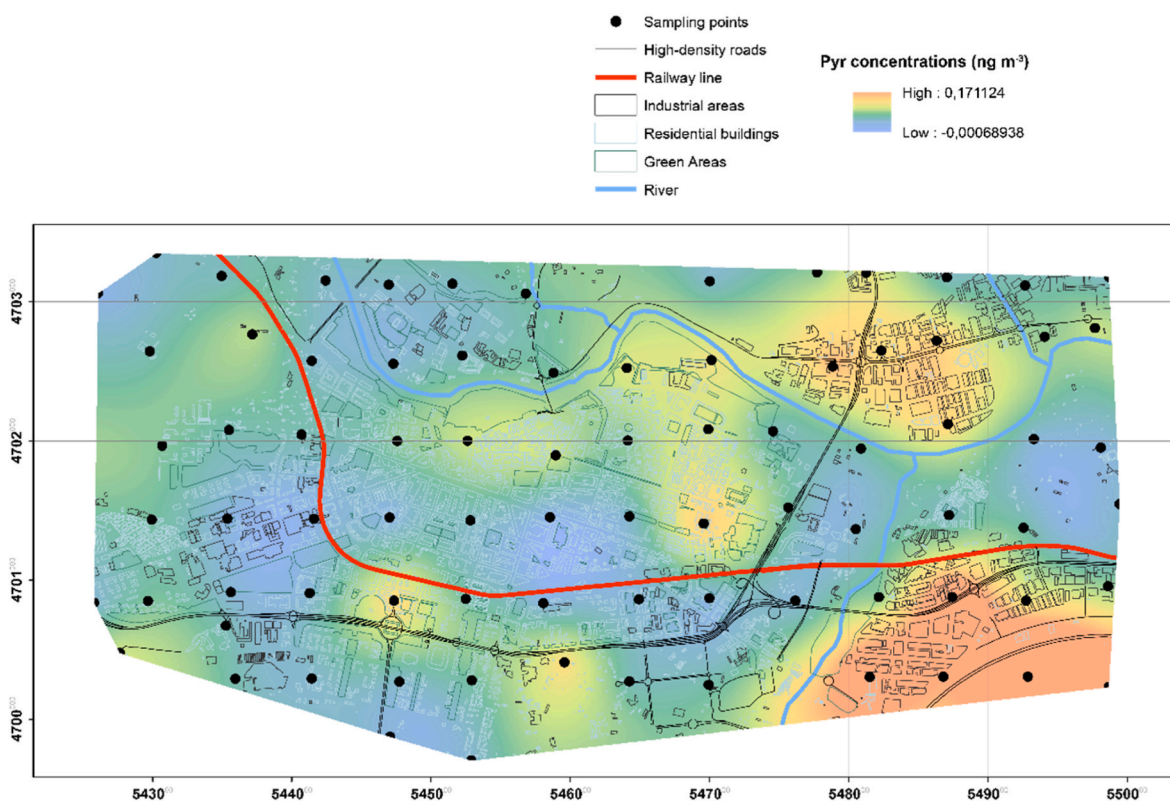

Fig. 4. Pollution map for the city of Logroño (N Spain). The map was produced by kriging of pyrene (Pyr) concentrations in PM_{10} (ng m^{-3}) estimated from the concentrations determined in Mosspheres. Reddish and bluish tones represent higher and lower concentrations of this compound, respectively.

However, concentration ranges attributed to fossil fuel combustion predominated in them (Figs. 8–10SM), indicating that this could be a major source of PAHs.

4. Discussion

4.1. PAH levels

Median concentrations of the total PAHs were 0.125 ng g^{-1} in Mosspheres, 0.142 µg m^{-2} d^{-1} in BD and 0.541 ng m^{-3} in PM$_{10}$. For individual PAHs, median concentrations ranged, from 0.001 to 0.028 ng g^{-1} in Mosspheres, from 0.001 to 0.045 µg m^{-2} d^{-1} in BD and from 0.006 to 0.285 ng m^{-3} in PM$_{10}$. The accumulation of 3-ring PAHs were 2–3 times higher than the sums of 4-, 5- and 6-ring PAHs in the Mosspheres, which can be explained by the easier diffusion of 3-ring PAHs through the sorbent material and their higher concentrations in the environment (Estellano et al., 2012; Mętrak et al., 2016; Wu et al., 2023). BaPyr concentrations were always below the legal limit of 1 ng m^{-3} in PM$_{10}$ (EU Directive, 2004/107/EC) and low TEQ values were obtained. Thus, the concentration of DBahAnt, (the PAH compound with the highest TEF: 5-fold the toxicity of BaPyr) was below the LOQ (1 ng g^{-1}) in 51% of the samples (Table 1), indicating the absence of high levels of this compound at most of the sampling points. Moreover, kernel distributions showed few PAH enriched points (Fig. 2 for PM10 and Fig. 1SM for BD).

The results show that the city of Logroño was not significantly affected by PAH pollution in the spring season. Accordingly, low PAHs concentrations, similar to those obtained in the Mosspheres in this study were found in the city in leaves of the ornamental tree *Ligustrum lucidum* in a regional report, for the same period (spring 2018; median total PAHs concentration 0.192 µg g^{-1}, median BaPyr concentration 0.002 µg g^{-1}; (Martínez-Abaigar et al., 2018). Likewise, in 2016, a biomonitoring study using the moss *Hypnum cupressiforme* detected low PAHs concentrations across the region (La Rioja, median total PAHs concentration 0.042 µg g^{-1}; Frontasyeva et al., 2020).

The concentrations obtained were lower than those obtained in Mosspheres in a previous study carried out in urban areas (higher populated than the city of this study) and in agricultural, background and industrial environments (Aboal et al., 2020), that found maximum values up to one order of magnitude higher (6.28 µg m^{-2} day^{-1} in BD and 6.98 ng m^{-3} in PM$_{10}$ for total PAHs). Additionally, much higher concentrations were found in moss of the same genus (*Sphagnum*) exposed during 3 months in a slightly smaller city (Opole, Poland) (0.144 µg g^{-1} as the median of BaPyr; Świsłowski et al., 2021). Likewise, concentrations 6 times higher were obtained in PM$_{10}$ using PUF in a turkish city with twice the population of Logroño (96.44 ng m^{-3} and 0.19 ng m^{-3} for total PAHs and BaPyr respectively, Dumanoglu et al., 2017) and 4 times higher using high volume air samplers in the rural area of the Tibetean Plateau (2.015 ng m^{-3} for total PAHs, Wu et al., 2023). Given that sources of PAH emissions usually release other pollutants simultaneously, the low PAH levels could also indicate generally good air quality in the study area.

In addition, the results demonstrated the high sensitivity of the Mosspheres, with limits of quantification in the order of 1 ppb or less (Table 1), that allowed the technique to discriminate between low levels of PAHs (see Tables 2 and 2SM). Even though the legislated limits of 1 ng m^{-3} are far above these values, a high sensitivity of the technique is essential in the context of growing public concern about pollution (Yin et al., 2020).

4.2. Spatial distribution of PAHs in the study area

Although the PAH levels were generally low, higher levels of the different PAHs were consistently observed at some sampling stations (e.g. 77, 66, 22, 47, 63, 75, 78 and 40). The dominance of westerly winds may lead to greater accumulation of pollutants in the Mosspheres located in the east of the city (https://es.windfinder.com/windstatistics/logrono-agoncillo). However, the stations characterised by high PAH levels were mainly associated with busy roads and industrial facilities, indicating that vehicular and industrial emissions are the major sources of PAHs in the study area (Figs. 1–2 and 1SM). This is supported by the diagnostic ratios obtained, that showed ranges compatibles with fossil fuel combustion as the predominant source (Figs. 8–10 SM). These sources are well-known sources of PAHs emissions (Shimada et al., 2022; Wu et al., 2023) and, therefore, it can be concluded that the Mosspheres were able to detect the sources of pollution. This is especially important for other monitoring areas for which we have no prior information regarding their industrial or road activities.

Because of the high sensitivity of the Mossphere technique, spatial structure in the concentrations of Pyr, BaPyr, BePyr, BghiPer and the sums of 5- and 6-ring PAHs was detected in the established sampling grid (side 575 m), thus enabling the construction of pollution maps for these compounds by spatial interpolation. These maps revealed that industry and vehicle emissions did not severely affect the air quality in residential areas and that the inhabitants were therefore exposed to relatively low levels of these pollutants (Figs. 3–4 and 5–6SM).

However, spatial structure was not observed in the concentrations of most of the PAHs (see Figs. 2-3SM). This may be explained by the presence of diffuse pollution sources, also underlined by the lack of a clear pattern in PAH diagnostic ratios. Diffuse sources may create a spatial structure at smaller scales than the established sampling interval (575 m) and thus be overlooked. This is not surprising, as variability in pollution levels at a local scale is widely documented (Anastasopoulos et al., 2012). In this respect, the cost-effectiveness of the Mosspheres would enable the sampling density to be increased, thus yielding higher spatial resolution at smaller scales.

4.3. Advantages of the Mosspheres over conventional methods

One of the main problems when monitoring air pollution is the high specificity and cost of air quality instruments (e.g. space, maintenance, technical equipment, etc.) (Aboal et al., 2020; Augusto et al., 2013). Economic constraints usually result in a low density of pollution monitoring stations on which prediction of pollution over the whole study area depends, thus yielding poor spatial resolution. In addition, there is still a lack of monitoring stations in many rural and urban areas owing to this limitation (WAQI.Info: World Air Quality Index; https://waqi.info/es/). The Mosspheres overcome these limitations by being cost-effective and maintenance-free. This way, their use allows for more accurate measurement at a higher spatial resolution than would be possible using conventional techniques.

Thus, the Mosspheres are valuable complements of conventional measurement methods (i.e. air pumps and deposition collectors) and can help to determine where sampling stations should be located by identifying those points with the highest PAH concentration. The ability of moss transplants to detect pollution sources overlooked by the sampling stations was described by Ares et al. (2011), resulting in the change of location of these stations in the study area.

4.4. Mossphere limitations

Aboal et al. (2020) did not observe significant correlations between the concentrations of 3-ring PAHs in Mosspheres and those in PM$_{10}$ and BD, so transformation of these values was ruled out. The lack of correlation between the concentrations of pollutants in moss biomonitors and those measured in the environment by conventional methods has also been reported in metal pollution studies (e.g. Aničić et al., 2009; Ares et al., 2015). Although this may represent a limitation of Mosspheres in terms of quantitative risk assessment, qualitative assessment of these pollutants remains possible, and Mosspheres could still be useful for detecting pollution hotspots and identifying sources of emission of 3-ring PAHs.

In addition, some losses of these compounds may have occurred during the exposure of the Mosspheres because of washing rain, wind or solar radiation (Ma et al., 2013). Since Aboal et al. (2020) compared PAH concentrations in shelter and unsheltered Mosspheres showing that there were no significant differences between them for PAHs with 4 or more rings, it was decided to keep the Mosspheres unsheltered.

Moreover, wide seasonal variations in PAH concentrations have been documented, with the highest concentrations occurring in winter. The increase in emissions from home heating systems, together with the limited dispersion of pollutants due to temperature inversions and the decrease in PAH degradation by solar radiation, may explain this seasonal pattern (Foan et al., 2015; Tan et al., 2006; Thang et al., 2020). Although the present study was carried out in spring, similar studies should be repeated in other seasons, especially in winter.

Finally, according to Aboal et al. (2020), the Mosspheres explained ca. 50% and 70% of the concentrations of PM_{10} and BD measured by conventional techniques, respectively. There is therefore a part of this variability that is not being picked up by this technique.

5. Conclusions

In this study, a sampling grid of Mosspheres was established to monitor PAHs concentrations in a medium-sized city. Low PAHs concentrations and TEQ values were found and enrichment with PAHs was detected in a few points, showing that this area was not significantly affected by PAH pollution. Spatial structure was detected for some compounds, with the highest concentrations of these compounds detected in busy roads and industrial facilities. These results support the use of Mosspheres for quantification, monitoring and mapping of a wide range of PAH compounds. Because of its cost-effectiveness, high sensitivity, portability and ease of use, the Mossphere technique (which can also be used to monitor other potentially toxic elements) could become a very useful tool for public administrations, industries and environmental managers.

Credit author statement

Carme Pacín: Formal analysis, data curation, Writing-Original draft preparation and visualization. Javier Martínez-Abaigar: Conceptualization, methodology, investigation, funding adquisition and Writing- Review & Editing. Encarnación Núñez-Olivera: Conceptualization, methodology, investigation, funding adquisition and Writing- Review & Editing. Jesús R. Aboal: Conceptualization, methodology, investigation, funding adquisition and Writing- Review & Editing. J. Ángel Fernández: Conceptualization, methodology, investigation, funding adquisition and Writing- Review & Editing. Flavia De Nicola: Investigation and Writing-Review & Editing.

Funding sources

Declaration of competing interest

The authors declare that they have no known competing financial interests or personal relationships that could have appeared to influence the work reported in this paper.

Data availability

Data will be made available on request.

Acknowledgements

Appendix A. Supplementary data

Supplementary data to this article can be found online at https://doi.org/10.1016/j.envres.2023.115406.

References

Aboal, J.R., Concha-Graña, E., De Nicola, F., Muniategui-Lorenzo, S., López-Mahía, P., Giordano, S., Capozzi, F., Di Palma, A., Reski, R., Zechmeister, H., Martínez-Abaigar, J., Fernández, J.A., 2020. Testing a novel biotechnological passive sampler for monitoring atmospheric PAH pollution. J. Hazard Mater. 381, 120949 https://doi.org/10.1016/j.jhazmat.2019.120949.

Alfonsín, C., Pérez-López, P., Rey-Asensio, A.I., Carballeira, C., Feijoo, G., Moreira, M.T., 2015. Assessing the environmental performance of a new biotechnological sensor for air quality based on devitalized moss clone. Environ. Res. Eng. Manag. 71, 56–67. https://doi.org/10.5755/j01.erem.71.1.10820.

Anastasopoulos, A.T., Wheeler, A.J., Karman, D., Kulka, R.H., 2012. Intraurban concentrations, spatial variability and correlation of ambient polycyclic aromatic hydrocarbons (PAH) and PM2.5. Atmos. Environ. 59, 272–283. https://doi.org/10.1016/J.ATMOSENV.2012.05.004.

Aničić, M., Tasić, M., Frontasyeva, M.V., Tomašević, M., Rajšić, S., Mijić, Z., Popović, A., 2009. Active moss biomonitoring of trace elements with Sphagnum girgensohnii moss bags in relation to atmospheric bulk deposition in Belgrade, Serbia. Environ. Pollut. 157, 673–679. https://doi.org/10.1016/j.envpol.2008.08.003.

Ares, A., Aboal, J., Carballeira, A., Fernández, J.A., 2015. Do moss bags containing devitalized Sphagnum denticulatum reflect heavy metal concentrations in bulk deposition? Ecol. Indicat. 50, 90–98. https://doi.org/10.1016/j.ecolind.2014.10.030.

Ares, A., Aboal, J.R., Carballeira, A., Giordano, S., Adamo, P., Fernández, J.A., 2012. Moss bag biomonitoring: a methodological review. Sci. Total Environ. 432, 143–158. https://doi.org/10.1016/J.SCITOTENV.2012.05.087.

Ares, Á., Fernández, J.Á., Aboal, J.R., Carballeira, A., 2011. Study of the air quality in industrial areas of Santa Cruz de Tenerife (Spain) by active biomonitoring with Pseudoscleropodium purum. Ecotoxicol. Environ. Saf. 74, 533–541. https://doi.org/10.1016/j.ecoenv.2010.08.019.

Aslam, R., Sharif, F., Baqar, M., Shahzad, L., 2022. Source identification and risk assessment of polycyclic aromatic hydrocarbons (PAHs) in air and dust samples of Lahore City. Sci. Rep. 121 12, 1–15. https://doi.org/10.1038/s41598-022-06437-8.

Augusto, S., Máguas, C., Branquinho, C., 2013. Guidelines for biomonitoring persistent organic pollutants (POPs), using lichens and aquatic mosses – a review. Environ. Pollut. 180, 330–338. https://doi.org/10.1016/j.envpol.2013.05.019.

Beike, A.K., Spagnuolo, V., Lüth, V., Steinhart, F., Ramos-Gómez, J., Krebs, M., Adamo, P., Rey-Asensio, A.I., Fernández, J.A., Giordano, S., Decker, E.L., Reski, R., 2014. Clonal in vitro propagation of peat mosses (Sphagnum L.) as novel green resources for basic and applied research. Plant Cell Tissue Organ Cult. 120, 1037–1049. https://doi.org/10.1007/S11240-014-0658-2.

Bivand, R.S., Pebesma, E., Gómez-Rubio, V., 2013. Applied Spatial Data Analysis with R. Springer, New York. https://doi.org/10.1007/978-1-4614-7618-4.

Capozzi, F., Giordano, S., Aboal, J.R., Adamo, P., Bargagli, R., Boquete, T., Di Palma, A., Real, C., Reski, R., Spagnuolo, V., Steinbauer, K., Tretiach, M., Varela, Z., Zechmeister, H., Fernández, J.A., 2016. Best options for the exposure of traditional and innovative moss bags: a systematic evaluation in three European countries. Environ. Pollut. 214, 362–373. https://doi.org/10.1016/j.envpol.2016.04.043.

Capozzi, F., Sorrentino, M.C., Di Palma, A., Mele, F., Arena, C., Adamo, P., Spagnuolo, V., Giordano, S., 2020. Implication of vitality, seasonality and specific leaf area on PAH uptake in moss and lichen transplanted in bags. Ecol. Indicat. 108, 105727 https://doi.org/10.1016/J.ECOLIND.2019.105727.

Carrieri, V., Fernández, J.Á., Aboal, J.R., Picariello, E., De Nicola, F., 2021. Accumulation of polycyclic aromatic hydrocarbons in the devitalized aquatic moss Fontinalis antipyretica: from laboratory to field conditions. J. Environ. Qual. 50, 1196–1206. https://doi.org/10.1002/JEQ2.20267.

Choi, S.-D., Kwon, H.-O., Lee, Y.-S., Park, E.-J., Oh, J.-Y., 2012. Improving the spatial resolution of atmospheric polycyclic aromatic hydrocarbons using passive air samplers in a multi-industrial city. J. Hazard Mater. 241–242, 252–258. https://doi.org/10.1016/j.jhazmat.2012.09.039.

Concha-Graña, E., Muniategui-Lorenzo, S., De Nicola, F., Aboal, J.R., Rey-Asensio, A.I., Giordano, S., Reski, R., López-Mahía, P., Prada-Rodríguez, D., 2015. Matrix solid phase dispersion method for determination of polycyclic aromatic hydrocarbons in moss. J. Chromatogr. A 1406, 19–26. https://doi.org/10.1016/J.CHROMA.2015.06.014.

Dumanoglu, Y., Gaga, E.O., Gungormus, E., Sofuoglu, S.C., Odabasi, M., 2017. Spatial and seasonal variations, sources, air-soil exchange, and carcinogenic risk assessment for PAHs and PCBs in air and soil of Kutahya, Turkey, the province of thermal power plants. Sci. Total Environ. 580, 920–935. https://doi.org/10.1016/J.SCITOTENV.2016.12.040.

Environment Protection Authority, 2021. Advisory Note- Classification of Policiclic Aromatic Hydrocarbons [WWW Document]. URL.

Estellano, V.H., Pozo, K., Harner, T., Corsolini, S., Focardi, S., 2012. Using PUF disk passive samplers to simultaneously measure air concentrations of persistent organic pollutants (POPs) across the Tuscany region. Italy. Atmos. Pollut. Res. 3, 88–94. https://doi.org/10.5094/APR.2012.008.

Foan, L., Domercq, M., Bermejo, R., Santamaría, J.M., Simon, V., 2015. Mosses as an integrating tool for monitoring PAH atmospheric deposition: comparison with total deposition and evaluation of bioconcentration factors. A year-long case-study. Chemosphere 119, 452–458. https://doi.org/10.1016/j.chemosphere.2014.06.071.

Frontasyeva, M., Harmens, H., Uzhinskiy, A., Chaligava, O., 2020. Mosses as Biomonitors of Air Pollution: 2015/2016 Survey on Heavy Metals, Nitrogen and POPs in Europe and beyond. Report of the ICP Vegetation Moss Survey Coordination Centre. Joint Institute for Nuclear Research, Dubna, Russian Federation, p. 136 participants of hte moss survey.

Gräler, B., Pebesma, E., Heuvelink, G., 2016. Spatio-temporal interpolation using gstat. R J 8, 204–218. https://doi.org/10.32614/RJ-2016-014.

Harmens, H., Norris, D.A., Koerber, G.R., Buse, A., Steinnes, E., Rühling, Å., 2007. Temporal trends in the concentration of arsenic, chromium, copper, iron, nickel, vanadium and zinc in mosses across Europe between 1990 and 2000. Atmos. Environ. 41, 6673–6687. https://doi.org/10.1016/j.atmosenv.2007.03.062.

Jovan, S.E., Monleon, V.J., Donovan, G.H., Gatziolis, D., Amacher, M.C., 2021. Small-scale distributions of polycyclic aromatic hydrocarbons in urban areas using geospatial modeling: a case study using the moss Orthotrichum lyellii in Portland, Oregon. U.S.A. Atmos. Environ. 256, 118433 https://doi.org/10.1016/j.atmosenv.2021.118433.

Kim, K.H., Jahan, S.A., Kabir, E., Brown, R.J.C., 2013. A review of airborne polycyclic aromatic hydrocarbons (PAHs) and their human health effects. Environ. Int. 60, 71–80. https://doi.org/10.1016/j.envint.2013.07.019.

Ma, W.L., Qi, H., Baidron, S., Liu, L.Y., Yang, M., Li, Y.F., 2013. Implications for long-range atmospheric transport of polycyclic aromatic hydrocarbons in Lhasa, China. Environ. Sci. Pollut. Res. 20, 5525–5533. https://doi.org/10.1007/S11356-013-1577-1/FIGURES/5.

Martínez-Abaigar, J., Núñez-Olivera, E., Tomás, R., Monforte, L., Soriano, G., del Castillo, M.Á., Carballeira, A., Aboal, J.R., Fernández, J.Á., 2018. Servicio de Investigación sobre Biomonitorización de Contaminación por Metales Pesados en el Área Metropolitana de Logroño. https://www.larioja.org/medio-ambiente/es/calidad-aire-cambio-climatico/calidad-aire/red-biomonitarizacion-metales-pesados-rioja/red-biomonitorizacion-metales-pesados-rioja.

Martinez-Swatson, K., Mihály, E., Lange, C., Ernst, M., Dela Cruz, M., Price, M.J., Mikkelsen, T.N., Christensen, J.H., Lundholm, N., Rønsted, N., 2020. Biomonitoring of polycyclic aromatic hydrocarbon deposition in Greenland using historical moss herbarium specimens shows a decrease in pollution during the 20th century. Front. Plant Sci. 11, 1085. https://doi.org/10.3389/fpls.2020.01085.

Mętrak, M., Aneta, E., Wiłkomirski, B., Staszewski, T., Suska-Malawska, M., 2016. Interspecific differences in foliar 1 PAHs load between Scots pine, birch, and wild rosemary from three polish peat bogs. Environ. Monit. Assess. 188, 456. https://doi.org/10.1007/S10661-016-5465-2.

Montaño-Soto, M.T., Garza-Ocañas, L., 2014. Health effects due to exposure to polycyclic aromatic hydrocarbons from the petroleum reining industry. Med. Univ. 16, 136–140.

Nisbet, I.C.T., Lagoy, P.K., 1992. Toxic equivalency factors (TEFs) for polycyclic aromatic hydrocarbons (PAHs). Regul. Toxicol. Pharmacol. 16, 290–300. https://doi.org/10.1016/0273-2300(92)90009-X.

Patel, A.B., Shaikh, S., Jain, K.R., Desai, C., Madamwar, D., 2020. Polycyclic aromatic hydrocarbons: sources, toxicity, and remediation approaches. Front. Microbiol. 11, 2675. https://doi.org/10.3389/FMICB.2020.562813/BIBTEX.

Pérez-Fernández, B., Viñas, L., Bargiela, J., 2018. Occurrence and toxicological assessment of polycyclic aromatic hydrocarbons (PAHs) in marine sediments under mussel farming influence. Environ. Sci. Pollut. Res. 25, 15862–15872. https://doi.org/10.1007/S11356-018-1737-4.

Qu, C., De Vivo, B., Albanese, S., Fortelli, A., Scafetta, N., Li, J., Hope, D., Cerino, P., Pizzolante, A., Qi, S., Lima, A., 2021. High spatial resolution measurements of passive-sampler derived air concentrations of persistent organic pollutants in the Campania region, Italy: implications for source identification and risk analysis. Environ. Pollut. 286, 117248 https://doi.org/10.1016/j.envpol.2021.117248.

Ravindra, K., Sokhi, R., Van Grieken, R., 2008. Atmospheric polycyclic aromatic hydrocarbons: source attribution, emission factors and regulation. Atmos. Environ. 42, 2895–2921. https://doi.org/10.1016/j.atmosenv.2007.12.010.

Shimada, K., Nohchi, M., Maeshima, K., Uchino, T., Kobayashi, Y., Ono, K., Ogata, H., Katsumi, N., Inazu, K., Okochi, H., 2022. Effects of changes in polycyclic aromatic hydrocarbons (PAHs) emissions and degradation on their concentrations in Tokyo from 2007 and 2016. Sci. Rep. 121 12, 1–9. https://doi.org/10.1038/s41598-022-08138-8, 2022.

Świsłowski, P., Hrabák, P., Wacławek, S., Liskova, K., Antos, V., Rajfur, M., Ząbkowska-Wacławek, M., 2021. The application of active biomonitoring with the use of mosses to identify polycyclic aromatic hydrocarbons in an atmospheric aerosol. Molecules 26, 7258. https://doi.org/10.3390/molecules26237258.

Tan, J.H., Bi, X.H., Duan, J.C., Rahn, K.A., Sheng, G.Y., Fu, J.M., 2006. Seasonal variation of particulate polycyclic aromatic hydrocarbons associated with PM10 in Guangzhou, China. Atmos. Res. 80, 250–262. https://doi.org/10.1016/J.ATMOSRES.2005.09.004.

Thang, P.Q., Kim, S.J., Lee, S.J., Kim, C.H., Lim, H.J., Lee, S.B., Kim, J.Y., Vuong, Q.T., Choi, S.D., 2020. Monitoring of polycyclic aromatic hydrocarbons using passive air samplers in Seoul, South Korea: spatial distribution, seasonal variation, and source identification. Atmos. Environ. 229, 117460 https://doi.org/10.1016/j.atmosenv.2020.117460.

Verbruggen, E.M.J., 2012. Environmental Risk Limits for Polycyclic Aromatic Hydrocarbons (PAHs): for Direct Aquatic , Benthic , and Terrestrial Toxicity.

Vingiani, S., De Nicola, F., Purvis, W.O., Concha-Graña, E., Muniategui-Lorenzo, S., López-Mahía, P., Giordano, S., Adamo, P., 2015. Active biomonitoring of heavy metals and PAHs with mosses and lichens: a case study in the cities of naples and london. Water. Air. Soil Pollut 226, 240. https://doi.org/10.1007/s11270-015-2504-5.

Wang, Z., Ren, P., Sun, Y., Ma, X., Liu, X., Na, G., Yao, Z., 2013. Gas/particle partitioning of polycyclic aromatic hydrocarbons in coastal atmosphere of the north Yellow Sea, China. Environ. Sci. Pollut. Res. 20, 5753–5763. https://doi.org/10.1007/s11356-013-1588-y.

Wickham, H., 2009. ggplot2. Springer, New York. https://doi.org/10.1007/978-0-387-98141-3.

Wu, X., Sun, W., Huai, B., Wang, L., Han, C., Wang, Y., Mi, W., 2023. Seasonal variation and sources of atmospheric polycyclic aromatic hydrocarbons in a background site on the Tibetan Plateau. J. Environ. Sci. 125, 524–532. https://doi.org/10.1016/J.JES.2022.02.042.

Yin, P., Brauer, M., Cohen, A.J., Wang, H., Li, J., Burnett, R.T., Stanaway, J.D., Causey, K., Larson, S., Godwin, W., Frostad, J., Marks, A., Wang, L., Zhou, M., Murray, C.J.L., 2020. The effect of air pollution on deaths, disease burden, and life expectancy across China and its provinces, 1990–2017: an analysis for the Global Burden of Disease Study 2017. Lancet Planet. Health 4, e386–e398. https://doi.org/10.1016/S2542-5196(20)30161-3/ATTACHMENT/00883166-FEE0-47C4-B6DD-9D72738374DC/MMC2.PDF.

Yunker, M.B., Macdonald, R.W., Vingarzan, R., Mitchell, R.H., Goyette, D., Sylvestre, S., 2002. PAHs in the Fraser River basin: a critical appraisal of PAH ratios as indicators of PAH source and composition. Org. Geochem. 33, 489–515. https://doi.org/10.1016/S0146-6380(02)00002-5.

Zhan, L., Huang, H., Zhao, S., Wang, Z., Zhang, G., Cheng, H., 2022. Comparison of atmospheric polycyclic aromatic hydrocarbons (PAHs) over six years at a CAWNET background site in central China: changes of seasonal variations and potential sources. Chemosphere 299, 134298. https://doi.org/10.1016/J.CHEMOSPHERE.2022.134298.